# CONCEPTUAL MODEL UPDATE FOR THE ROTOKAWA GEOTHERMAL FIELD, NEW ZEALAND

Aimee Calibugan[1], Kelly Melia[1], and Manuel Rivera[1]

[1] Mercury Ltd, 283 Vaughan Rd, Rotorua 3010, New Zealand

Aimee.Calibugan@mercury.co.nz

**Keywords:** *Rotokawa, conceptual model*

## ABSTRACT

This paper presents the updated conceptual understanding of the Rotokawa geothermal field, which is located within the Taupo Volcanic Zone, New Zealand. The Rotokawa geothermal field has an installed capacity of 174 MWe and is a joint venture between Mercury NZ Ltd and Tauhara North No. 2 Trust. Analyses of the data obtained from additional make-up well drilling, updates on the field stratigraphy, and the detailed review of the field and individual well performance 10 years since the Nga Awa Purua plant commissioning, have led to changes in the conceptualised field reservoir geometry, upflow location, deep hydrology of the system, and connectivity to the overlying intermediate aquifer.

## 1 INTRODUCTION

The Rotokawa geothermal field is one of the hottest geothermal resources within the Taupo Volcanic Zone (TVZ). It is currently producing 174 MWe with 12 production wells and 6 injection wells. The field operation is jointly managed by Tauhara North No. 2 Trust and Mercury NZ Ltd, operating as Rotokawa Joint Venture Ltd (RJV).

The Rotokawa power station (RKA) was first commissioned in 1997 at 24 MWe which was subsequently upgraded to 34 MWe. The Rotokawa field capacity was increased to 174 MWe with the coming online of the Nga Awa Purua (NAP) plant in 2010. Pogacnik et al. (2019) provides a lookback on Rotokawa geothermal field's 20 years of operation.

The conceptual model of Rotokawa has evolved since the 2015 conceptual and numerical model updates by Sewell et al. (2015) and Hernandez et al. (2015), respectively. The latest version of this conceptual model is described herein.

## 2 ADDITIONAL DATA SINCE THE 2015 MODEL

This paper summarises updates to the conceptual model that have been made using additional data collected between 2015 and 2020. The conceptual model update presented in this paper has served as a basis for the latest full-field reservoir model update, i.e., Rotokawa Reservoir Model V6.1 (Rivera, 2021).

### 2.1 Well Drilling

RK35 was drilled in 2016 in the northern part of the field. The successful drilling and good well output of RK35 have confirmed viability of the northern area.

RK36, drilled in 2017, is the largest production well in the field and initially produced >900 t/h. Well production and fluid chemistry data confirmed that this area of the reservoir is receiving pressure support (and probably recharge?) from injection. The large capacity of the well enabled a significant reduction in mass take for the western wells and subsequent pressure recovery.

RK37 was drilled in 2020 as a replacement well for RK14, which was abandoned in 2020 due to an external well casing corrosion issue. Heat-up surveys of the well confirmed temperature of up to 320 °C at the bottom of the well.

### 2.2 Field Stratigraphy and Structural Features

The stratigraphic interpretation of the field was also modified based on results of the additional analysis done on Rotokawa drill cuttings (Milicich et al., 2020). The key changes include the Rotokawa Andesite morphology which is now modelled as being emplaced as a 'sheet-like' flood andesite rather than modelled as a large composite cone. With the updated field stratigraphy, the Andesite Valley in the RK30/RK25 area has also been removed. The Haparangi Rhyolite was also changed to Oruahineawe Formation Rhyolite to represent a series of individual and coalesced rhyolitic domes that are collectively linked to the surficial Oruahineawe dome in the NE part of the field. Fulljames Rhyolite 1 & 2 have also been coined to refer to the petrographically distinct rhyolite lavas (Milicich et al., 2020) intersected by RK16, RK17, RK18, and RK27. Figure 10 shows a cross-section of the updated stratigraphy for Rotokawa.

Using the GNS database of active faults and the updated field stratigraphy, the structural features of Rotokawa were redrawn. Figure 9 shows the updated structural features of Rotokawa. Aratiatia Faults 6 & 7 have been added based on GNS database of active faults. The Production Field Fault in the west was removed as there is no longer stratigraphic justification for this. Based on the updated faults, there is now a NE-SW "graben" structure running through the production area at the centre of the field (Figure 1).

### 2.3 Post-2015 Production and Monitoring Data

#### 2.3.1 Reservoir Pressure

Heterogeneity in reservoir permeability is common across the Rotokawa reservoir as seen in the large variation in production capacity difference and pressure drawdown between wells. Figure 2 shows the well groupings based on variation in the measured reservoir pressure. Pressure drawdown resulting from the first stage of development (RKA) was moderate at less than 10 bar. With the NAP plant commissioning, the western group of wells experienced a large pressure drawdown, which was consistent and aligned in time among the wells in this group. On the other hand, the wells in the north group have only experienced a moderate pressure change. Wells in the central group also experienced a large pressure drawdown but at a much later period and as


ISSN 2703-4275

more of a response to the wells' own production. With the shift in higher production rates from the west to the north (Figure 3) after RK35 and RK36 drilling, recovery in reservoir pressure in the western region up to 20 bars in some wells was observed (Figure 4). Pressure changes at the deep injection area (wells RK20 to RK24) and the intermediate aquifer have been relatively small.

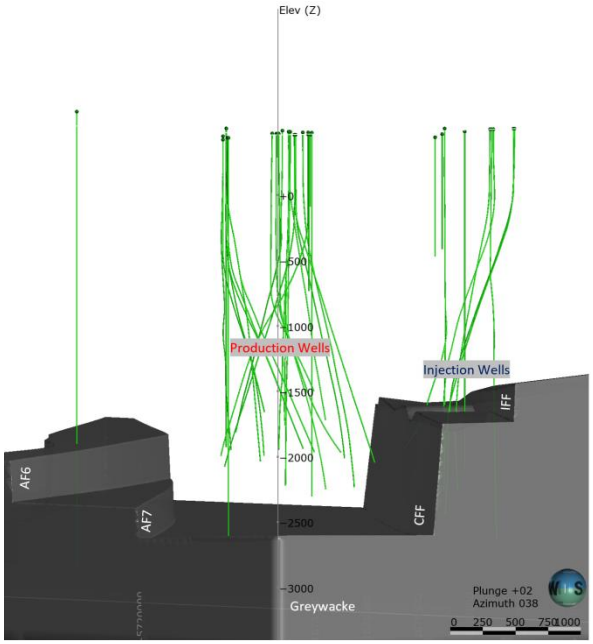


**Figure 1. The NE-SW graben running through the production area of the field. Note: CFF = Central Field Fault, IFF = Injection Field Fault, AF6 = Aratiatia Fault 6, and AF7 = Aratiatia Fault 7.**

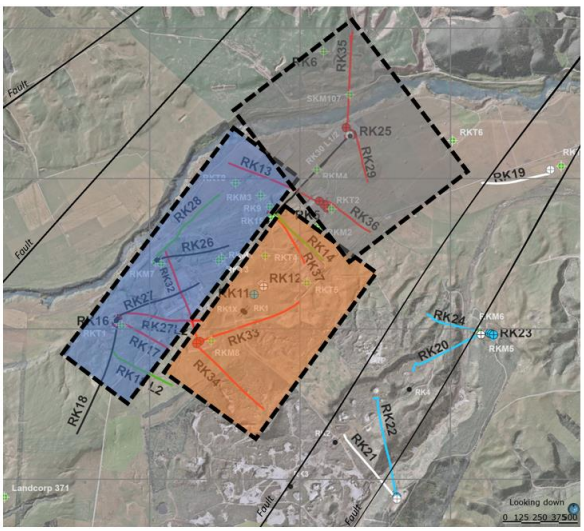


**Figure 2. Production well grouping based on reservoir pressure. West, Central, and Northern shown in blue, orange and grey, respectively. The main injection area is to the southeast. Refer to Figure 9 for the wellhead and well track color coding.**

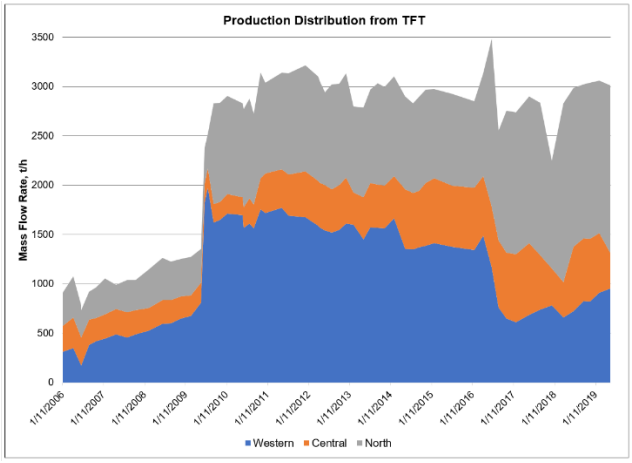


**Figure 3. Mass flow rate distribution based on Tracer Flow Testing (TFT) data.**

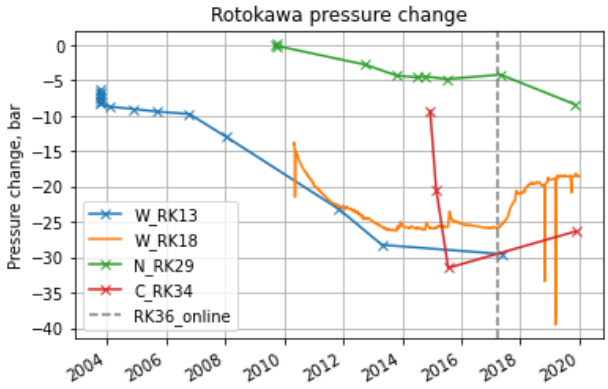


**Figure 4. Pressure drawdown from initial conditions at representative wells in the west, north and central groups.**

### 2.3.2 Reservoir Enthalpy

The average field enthalpy remained fairly stable at ca. 1550 kJ/kg between 1997 and 2009. The additional mass extraction requirement after the NAP plant commissioning has increased the average field enthalpy due to reservoir pressure drawdown and boiling process (i.e. an increased in-situ steam fraction) in the shallower depths of the production area. This boiling process was transient, and after 2011, a re-saturation process occurred as reflected in the decreasing trend in field enthalpy. Virtually no cooling has been observed up to 2020 in the deeper compressed-liquid depth of the reservoir, which indicates that most, if not all, of the observed enthalpy decline is confined only in the two-phase zone. Currently, the enthalpy decline is relatively small field-wide, averaging at ~0.2%/yr based on the mass-weighted TFT measurements Figure 5.

This boiling and re-saturation sequence of processes has been observed in the western and central group of wells only. In the north, the area which contains some of the highest permeability and highest flow capacity wells like RK29 and RK36, enthalpy has remained relatively unchanged with minimal to no excess enthalpy.


ISSN 2703-4275

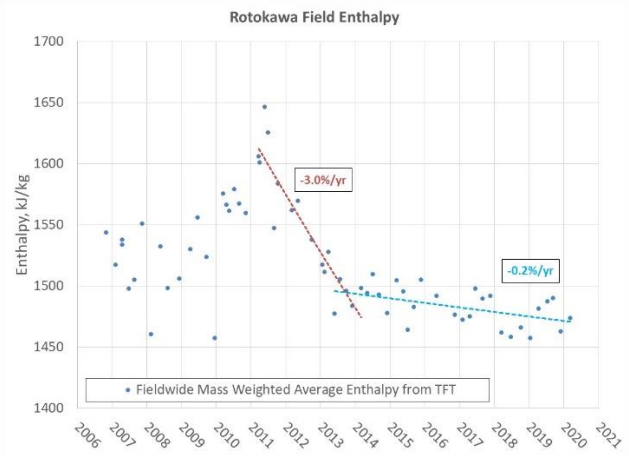


**Figure 5. The field mass weighted average enthalpy from TFT measurements.**

### 2.3.3 Fluid Chemistry

Since 2015, production well geochemistry monitoring has shown some clear chemistry changes in different areas of the reservoir. In general, the chemistry responses identify three different zones of the production area which are variably affected by boiling, injection breakthrough, and marginal recharge. These areas (Figure 6) are identified as:

- Central Zone (including RK5, RK14, RK29, RK33, RK34, and RK36) which are principally showing indications of high chloride rechange, including injection returns.
- Northern Zone (including RK13 and RK35) showing indications of stable reservoir processes.
- Western Zone (including RK17, RK26, RK27L2, RK28, and RK32) showing influence of mixing with marginal fluids.

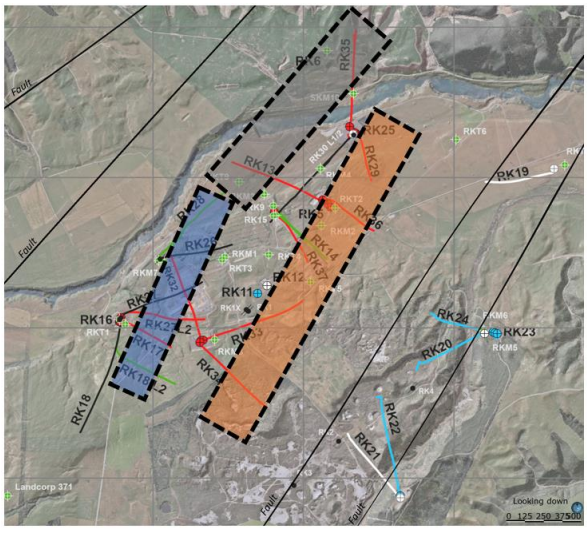


**Figure 6. Production well grouping based on discharge chemistry. West, Central, and Northern shown in blue, orange, and grey, respectively. Refer to Figure 9 for the wellhead and well track color coding.**

It is noteworthy that areas of consistent chemistry responses do not always coincide with the defined pressure regions as illustrated above in Figure 2.

Wells in the Central Geochemistry Zone have been observed to increase in chloride concentration and decline in non-condensable gases concentration since NAP start-up. Based on results from the reservoir tracer tests, it is now known that at least some of these geochemical effects relate to chemical breakthrough from brine injection. The NAP brine injectate chloride is concentrated and degassed as a result of the triple flash processing, as such injection support would result in an increase in chloride concentration and a decrease in NCG concentration. Two reservoir tracer tests have been conducted using a thermally stable isotope of iodine ($^{125}$I), one in mid-2013 on RK24 and another in late-2015 on RK22 (Addison et al., 2017).

Boiling was initially a significant influence in the area around RK17 and RK27, likely because of the large pressure drawdown. The wells initially had strongly increasing chloride and declining non-condensable gas concentrations, along with an increasing steam fraction at the wellhead. The possibility of a high chloride recharge in the shallow reservoir horizon originating from boiled upflow has been hypothesised to explain the rapid increase in the concentration of chemical analytes, especially chloride, in the early production at RK17 and 27. This is because boiling alone cannot account for the chloride increase observed during this period or injection return, as reservoir tracer tests in 2013 and 2015 have not shown tracer returns in this area within a one-year timeframe.

The discharge fluid of western wells indicates evidence of increased dilution, initially at RK28 and RK26, moving further in-field in more recent times. Marginal recharge previously seen in RK28 and RK26 has now likely reached RK17, RK27 and RK32 to some extent. This marginal fluid is cooler than the reservoir, with an elevated sulphate concentration and relatively low chloride concentration. Conceptually, this is considered to be downflowing through an Aratiatia fault (6 or 7).

Wells in the Northern production area (RK13 and RK35) exhibit generally stable chemistry with dilute chloride (around 500 ppm), high sulphate (15 ppm), and relatively low geothermometer temperatures (310 °C). RK25 also exhibits generally stable behaviour, however reduced permeability in this area gives rise to fluctuations in well chemistry.

## 3 CONCEPTUAL MODEL ELEMENTS

The key features of the latest Rotokawa conceptual model are summarised in Table 1. Figure 9 and Figure 10 illustrate the key elements of the latest conceptual model of the field.

**Table 1. Key Features of the Current Model**

| Element | Model Features |
|---|---|
| Upflow | - Single upflow, single phase liquid |
| Outflow | - Deep outflow to North<br>- Vertical shallow outflow through Central Field Fault to the intermediate aquifer<br>- Shallow outflow to the WNW (at natural-state) to the intermediate aquifer |
| Sources of recharge | - Deep lateral recharge from the west<br>- High chloride recharge |


ISSN 2703-4275

| | |
|---|---|
| | - Shallow Recharge from the West (or 'West Downflow') during Production State<br>- Injection returns |

### 3.1 Reservoir Geometry

The reservoir top and bottom of the Rotokawa deep geothermal reservoir model have largely remained unchanged since the 2015 field model by Sewell et al. (2015). However, the lateral boundaries of the field have been modified to integrate additional field data and interpretations.

The top of the Rotokawa deep geothermal reservoir varies from approximately -700 m to -1000 mRL. This is inferred primarily from the natural-state temperature gradients from well data, MT resistivity interpretation, and hydrothermal alteration mineralogy. The permeable reservoir is overlain with a low permeability 'cap' (Figure 10) which is associated with the smectite-rich portions of the Waiora Formation, Whakamaru Group Ignimbrite and in some areas in the Oruahinaewe Rhyolite.

The base of the reservoir has not been intersected by well drilling to date. The basement greywacke has been intercepted in nine Rotokawa wells, most of which are located in the southeast injection area of the field except for RK16, a deep well (with total depth of >3000 m) in the production area. Good permeability has been encountered in the greywacke units of the injection wells as verified by Pressure-Temperature-Spinner (PTS) data. The bottom of the Rotokawa geothermal reservoir is currently constrained primarily by microseismic data. Microseismic events at Rotokawa mainly correlate with the depth of injection zones.

The lateral extents of the reservoir have been delineated based on the interpretations of well characteristics to date (e.g. chemistry, enthalpy, and pressure drawdown), results of additional well drilling, updated field structures, and MT data. Figure 9 shows the proven resource boundary which is mainly delineated using a 300 m radius from the bottom of wells with high temperature and good permeability. The eastern boundary has been correlated with the Injection Field Fault based on the drilling results of RK23. Uncertainty on the southern reservoir boundary remains with MT data showing deepening clay cap south of RK21 and RK22 but this has not been confirmed by drilling.

The northeastern probable boundary has been modified based on results of RK35 drilling in 2016. RK35 is the northernmost production well of the field with stable well temperature, pressure and chemistry. The stable chemistry, enthalpy and minor pressure drawdown in the northern wells RK29, RK35 and RK36 compared to the rest of the production area indicates that the surrounding permeability is high and hot fluids recharge is abundant, likely from the upflow fluids but also from conductively heated injection returns mixed with upflow fluids.

### 3.2 Upflow

The conceptual model of Rotokawa assumes a single upflow towards the southern portion of the field where the hottest temperatures have been measured. This slightly differs from the 2015 conceptual model (Sewell et al., 2015) where either a single upflow or multiple upflows were proposed as feasible model for the field. Hernandez et al. (2015) used multiple upflows in the subsequent numerical model of the field. The main factors for invoking a single upflow model for the field are the temperature and chemical gradients at natural-state and that the numerical model was able to sufficiently match the well/field history using the simpler single upflow.

In the updated model, the upflowing fluid is inferred to have temperatures of up to 340 °C with chloride concentrations of 700 ppm and a gas content of 2 wt% in total fluid based on mixing models. RK4 is still the best characterisation of the upflow but the relatively low temperature and gas suggests the fluid reaching RK4 is likely boiled. RK2 and RK3 are much shallower (around 1000 mD) and show highly boiled chemistry signatures (i.e. not representative of the upflow). RK4 has limited data (one of the first crown wells) dating back to the 1980s.

### 3.3 Deep Outflow to the North

This is inferred from the observed natural-state temperature (Figure 7), geochemical gradients (i.e. decreasing temperature trends from south to north coupled with more dilute chloride trends from south to north) and the relatively stable pressure, enthalpy and chemistry of northern wells RK29, RK35 and RK36. This deep outflow to the northeast is consistent with the 2015 model by Sewell et al. (2015).

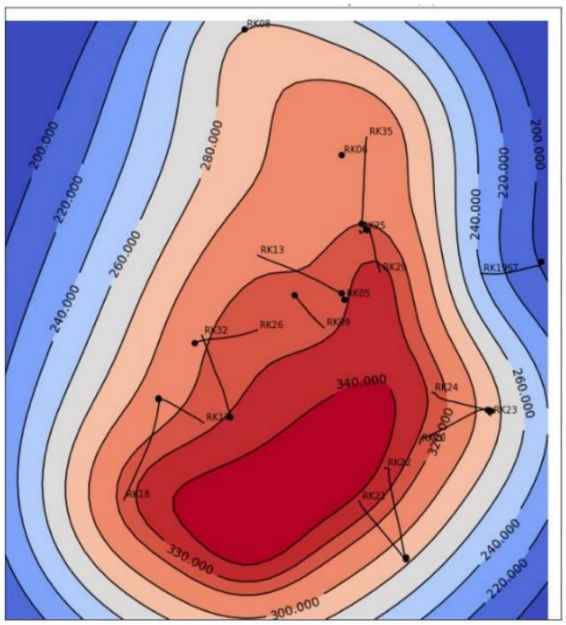


**Figure 7. A contour plot of the maximum observed well temperatures. Well tracks shown indicate the data used to constrain the contours.**

### 3.4 Deep Lateral Recharge from the West

The deep western lateral recharge is inferred from the natural-state temperature and chemical gradients, and the recharge is assumed to be entering the reservoir below the drilled depths. This recharge is inferred to have temperatures of about 280 °C based on mixing models. The source of this deep lateral recharge could be related to deep meteoric circulation and heating down the Aratiatia fault zone. This is a new feature to the Rotokawa conceptual model that was not discussed in the 2015 model (Sewell et al., 2015).


ISSN 2703-4275

### 3.5 Shallow Outflow to the WNW (Natural-State) / Shallow Recharge from the West (Production State)

In the natural state, this was an outflow of the deep reservoir into the intermediate aquifer towards the west-northwest but this is conceptualised to reverse flow direction during production, allowing marginal recharge into the reservoir (Figure 9). This reversal was caused by concentrated production and pressure drawdown in the west resulting in an influx of marginal recharge via the 'west downflow'. It is inferred that intermediate aquifer fluid downflows into the deep reservoir through Aratiatia Fault 6 and/or 7 then migrates laterally to the shallow zones of RK26/RK28 through good horizontal permeability causing the cooling observed in the shallow zones of RK26 and RK28. This flowpath is a new feature of the Rotokawa model that was not included in the Sewell et al. (2015) conceptual model.

### 3.6 Injection Flow Path

Tracer injection test results (e.g. 2013 and 2015) confirmed the connection between the deep injection wells in the southern part of the field to the central production area (Addison et al., 2017). The relatively low tracer recovery and long tracer arrival times indicate that the risk of thermal breakthrough from injection was relatively low at the time of the tests. In contrast to the previous model, the Central Field Fault (CFF) is not considered a hydraulic barrier anymore, but more a buffer to injection flow, with good along-strike and vertical permeability and less across-strike permeability. This is consistent with the microseismic data (Figure 8). High density clusters of microseismic events occurred initially on the eastern side of the CFF around the injection area then have progressed towards the production area on the western side of the CFF over time. This suggests the CFF is acting as a buffer to fluid flow slowing down migration of injection into the production area.

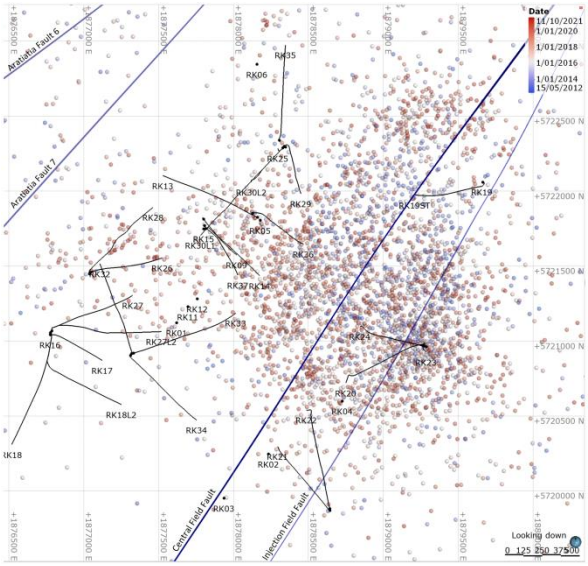


**Figure 8. Microseismic events over time.**

### 3.7 High Chloride Recharge

The high chloride recharge postulated in the updated conceptual model is formed in the shallow horizon of the deep production reservoir. This fluid can be represented by that sampled at RK3 in pre-production times, with ~1800 ppm chloride concentration and an enthalpy below 1200 kJ/kg. RK3 is sited above the proposed upflow area in an area of migration of boiling upwelling fluid, however this high chloride fluid is likely present in a wider area of the reservoir where boiling and steam migration to the intermediate aquifer/surface allow a concentration effect to occur in the liquid phase, as shown in Figure 10.

In production times it is suggested that this boiled fluid either migrates towards the southern area of the production zone or is generated near the southern production wells in response to pressure drawdown in the area. The observed effect is a rapid increase in chloride concentration in RK17 and RK27L2, which cannot be wholly explained by a simple near-well boiling process. Later wells RK33 and RK34 in this southern area also demonstrate similarly high chloride discharges to RK17 and RK27L2. The output from a process model for these wells demonstrated that the production of higher steam fractions associated with boiling in these wells would result in a maximum liquid phase chloride concentration of 700 ppm (at very high steam fractions). This is significantly below the observed chloride concentrations of around 1000 ppm at relatively moderate steam fractions. Therefore, a source of high chloride (boiled) fluid is required to match the chloride and enthalpy trends of these wells.

The lack of tracer returns from either $^{125}I$ reservoir tracer test to date (Addison, 2017) provides additional weight to this hypothesis.

### 3.8 Connection between Geothermal Reservoir and Intermediate Aquifer

There are two inferred key connection points between the reservoir and intermediate aquifer (Figure 10). The first is an outflow from the deep reservoir into the intermediate aquifer through the Central Field Fault in the southern portion of the field, as discussed by Sewell et al., (2015) in the 2015 conceptual model. The second is an outflow into the intermediate aquifer, in natural-state, towards the west-northwest and this then reverses flow direction, in response to production, bringing in marginal recharge into the reservoir, as discussed in Section 3.5.

### 3.9 Permeability

Permeability at Rotokawa appears to be highly heterogeneous, and the different pressure drawdown regions are associated with different permeability areas. These permeability areas influence the observed differences in well productivities. In addition, permeability at Rotokawa appears to have a strong degree of anisotropy, with preferential permeability along the strike of the local fault system and lower, but not null, permeability across-strike. This permeability anisotropy helps explain satisfactorily important observations in the field, such as the pattern of returns obtained during the reservoir tracer injection test, the strong recharge of hot fluids observed in the north of the field, the limited permeability at RK08, and the proposed deep discharge direction to the north-east of the field.

## 4 SUMMARY

This paper presents the latest conceptual understanding of the Rotokawa geothermal field that best fits the currently available data. Key changes in the conceptual model including the addition of new model features as discussed have been implemented in the current numerical model of the field.


ISSN 2703-4275

## 5 ACKNOWLEDGEMENTS

The authors thank the Rotokawa Joint Venture for allowing the publication of this data. Candice Bardsley is acknowledged for building the Rotokawa 3D earth model. Justin Pogacnik is also acknowledged for his contributions to the conceptual model update.

## 6 REFERENCES

Addison, S., Azwar, L., Clearwater, J., Hernandez, D., Mountain, B., Blair, A., and Siratovich, P. (2017). Improving the Conceptual Understanding Through a Recent Injection of 200 GBq of Iodine-125 at the Rotokawa Geothermal field, New Zealand. Proceedings 42nd Workshop on Geothermal Reservoir Engineering, Stanford, California, February 13-15, 2017.

Hernandez, Dario & Clearwater, Jonathon & Burnell, John & Franz, Peter & Azwar, Lutfhie & Marsh, Andrew. (2015). Update on the Modeling of the Rotokawa Geothermal System: 2010 – 2014.

Milicich, S.D., Chambefort, I., Simpson, M.P., Wilson, C.J.N., Alcaraz, S., Calibugan, A., Bardsley, C., and Morales, A.G. (2020). Geology, Geochronology, Alteration and Geochemistry of the Rotokawa Geothermal System, Taupo Volcanic Zone, New Zealand. Proceedings World Geothermal Congress 2020.

Pogacnik, J., Melia, K., Calibugan, A., Addison, S., Azwar, L., Jackson, M., Bardsley, C., Marsh, A., Wootton, D., and Stevens, M. (2019). A Lookback on 20 Years of Production at the Rotokawa Geothermal Field. European Geothermal Congress 2019, Den Haag, the Netherlands, 11-14 June 2019.

Rivera, M. (2021). Rotokawa Reservoir Model (RRM) v6.1, Report submitted to the Waikato Regional Council.

Sewell, S.M., Addison, S.J., Hernandez, D., Azwar, L., and Barnes, M.L. (2015). Rotokawa Conceptual Model 5 years After Commissioning of the 138 MWe NAP Plant. Proceedings 37th New Zealand Geothermal Workshop, 18-20 November 2015, Taupo, New Zealand.

Winick, J., Powell, T., Mroczek, E. (2011). The natural-state geochemistry of the Rotokawa reservoir. Proceedings New Zealand Geothermal Workshop 2011, Auckland, New Zealand.

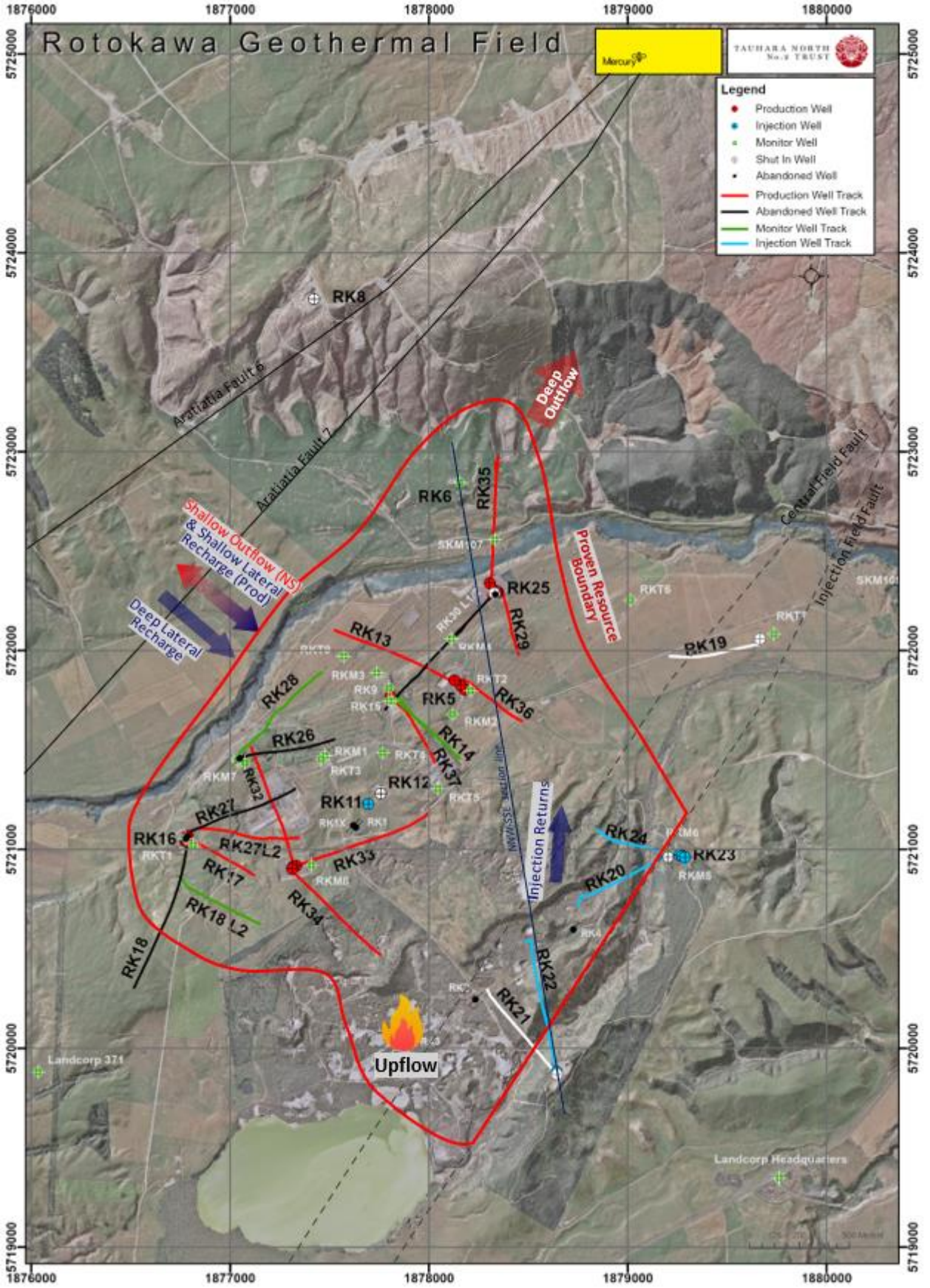


**Figure 9. Key elements of the Rotokawa conceptual model. The dashed lines for the Central Field Fault and Injection Field Fault indicate that these two faults are considered inactive faults.**



Proceedings 44th New Zealand Geothermal Workshop
23-25 November 2022
Auckland, New Zealand
ISSN 2703-4275

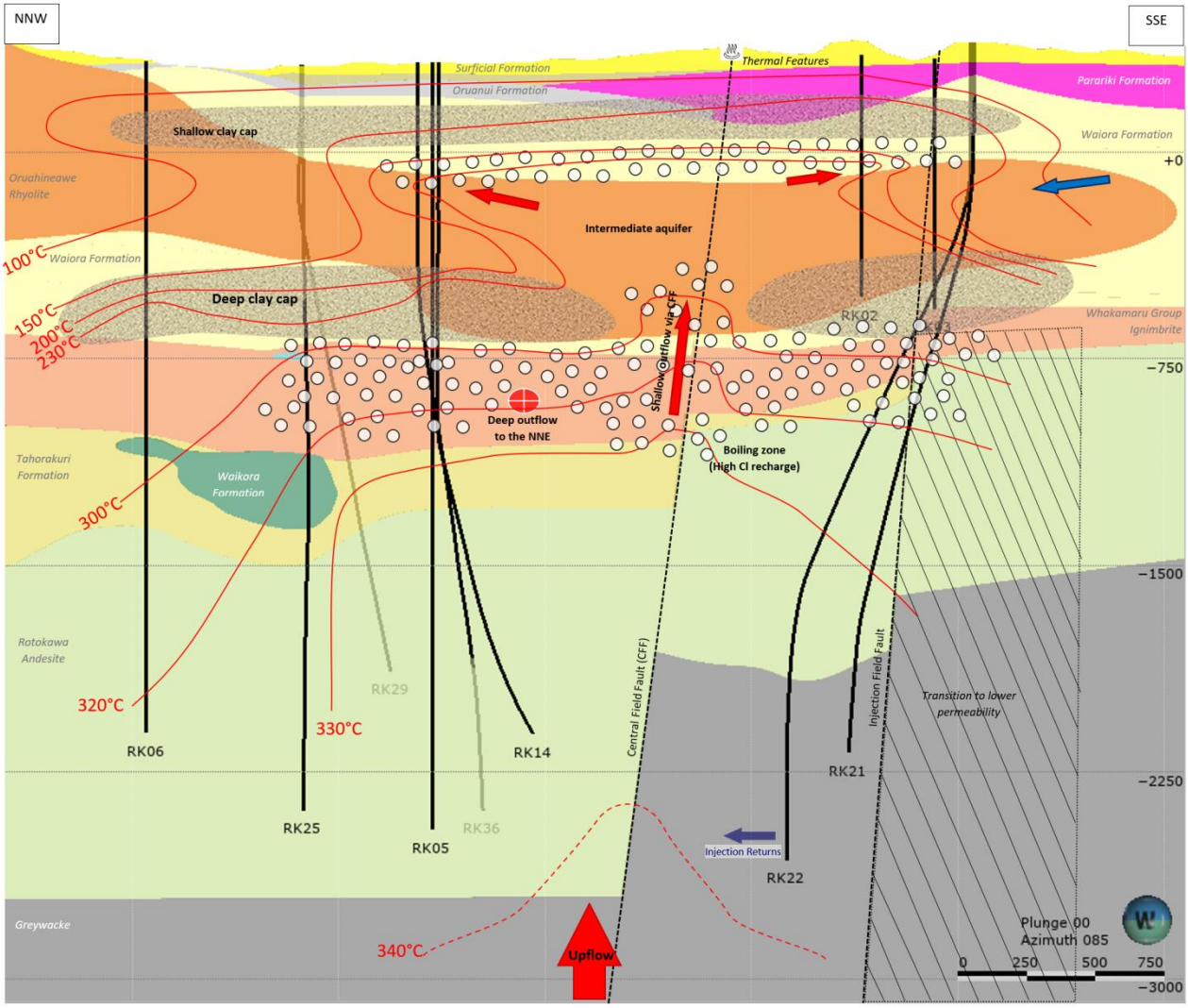


**Figure 10. 2D schematic of the Rotokawa conceptual model. Elements off-section not represented in the figure. Temperature contours are from natural-state.**



Proceedings 44th New Zealand Geothermal Workshop
23-25 November 2022
Auckland, New Zealand
ISSN 2703-4275